

Unraveling the couplings of a Drell-Yan produced Z' with heavy-flavor tagging

Wei-Shu Hou^{1,2}, Masaya Kohda¹, and Tanmoy Modak¹

¹*Department of Physics, National Taiwan University, Taipei 10617, Taiwan and*

²*ARC CoEPP at the Terascale, School of Physics, University of Melbourne, Vic 3010, Australia*

Despite no new physics so far at the LHC, a Z' boson with $m_{Z'} \sim 100$ GeV could still emerge via Drell-Yan (DY) production, $q\bar{q} \rightarrow Z' \rightarrow \mu^+\mu^-$, in the next few years. To unravel the nature of the Z' coupling, we utilize the c - and b -tagging algorithms developed by ATLAS and CMS to investigate $cg \rightarrow cZ'$ at 14 TeV LHC. While light-jet contamination can be eliminated, mistagged b -jets cannot be rejected in any of the tagging schemes we adopt. On the other hand, for nonzero bbZ' coupling, far superior b -tagging could discover the $bg \rightarrow bZ'$ process, where again light-jet mistag can be ruled out, but mistagged c -jets cannot yet be excluded. Provided that DY production is discovered soon enough, we find that a simultaneous search for $cg \rightarrow cZ'$ and $bg \rightarrow bZ'$ can conclusively discern the nature of Z' couplings involved.

I. INTRODUCTION

A Z' boson a few hundred GeV in mass could still emerge via the Drell-Yan (DY) process, $q\bar{q} \rightarrow Z' \rightarrow \mu^+\mu^-$, for qqZ' couplings that are weaker than analogous Standard Model (SM) couplings. Recent searches [1, 2] set stringent bounds on the couplings of such a Z' boson to u , d and s quarks, but the limits are much weaker for c or b quarks, hence discovery is possible within the next few years. One such scenario [3] involves a Z' that couples to c quarks, leading to DY production $c\bar{c} \rightarrow Z' \rightarrow \mu^+\mu^-$ at the LHC. The $cg \rightarrow cZ' \rightarrow c\mu^+\mu^-$ process then offers a unique probe of the flavor structure of the Z' coupling, if the c -jet flavor can be identified. Recent developments at ATLAS and CMS in c -tagging [4–6] algorithms and excellent performance of b -tagging [5, 7, 8] offer such an opportunity. In this paper we discuss how these heavy flavor taggers can probe the couplings of a Z' after its discovery through the DY process.

We illustrate with the scenario of Ref. [3], where a Z' couples relatively weakly to charm quarks and predominantly to muons. The DY process $pp \rightarrow Z' + X \rightarrow \mu^+\mu^- + X$ (X being inclusive activity) could emerge in the next few years, and a ccZ' coupling would imply the $cg \rightarrow cZ'$ process. We apply the c -tagging algorithms to investigate the discovery potential of $pp \rightarrow cZ' + X \rightarrow c\mu^+\mu^- + X$ (denoted as cZ' process, with the conjugate process implied) at $\sqrt{s} = 14$ TeV LHC.

The c -tagging algorithms of ATLAS [4, 5] and CMS [6] discriminate c -jets from light-jets (jets originating from u , d , s and gluon) at the expense of c -tag efficiency, while misidentification (or mistag) rate of b -jets as c -jets are relatively sizable. If the Z' couples to light $q = u, d, s$ quarks, a potential cZ' signal may arise from mistag (denoted as fake cZ'). As the qqZ' coupling is constrained by search for heavy resonance in DY process [1], our analysis shows that in certain c -tagging schemes one can completely rule out the possibility of fake cZ' from light-jets. But these tagging schemes fail to rule out the possibility of fake cZ' from mistagged b -jet.

In case the Z' couples instead to b quarks (bbZ' coupling), $pp \rightarrow bZ' + X \rightarrow b\mu^+\mu^- + X$ (bZ' process)

would emerge after the discovery in DY. This process could be observed by the well developed b -tagging algorithms [5, 7, 8], which provide excellent discrimination against light- and c -jets while maintaining high b -tagging efficiency. We find the current limit on ccZ' coupling allows for fake bZ' discovery at LHC due to mistag of c -jet as b -jet. However, this fake bZ' process at LHC could be ruled out if ~ 250 fb⁻¹ data is collected. We find that, if a Z' is discovered via the DY process in the next few years, combining the cZ' and bZ' signatures together with current limits from heavy resonance searches, one can conclusively infer the nature of Z' couplings.

We finally consider a case where both bbZ' and ccZ' couplings are nonzero and study DY, cZ' and bZ' processes for a representative Z' mass. We find that the coupling structure of such a scenario can also be disentangled, if combined with the current limit from heavy resonance search in DY process.

The paper is organized as follows. In Sec. II, we analyze the discovery potential of the DY process due to qqZ' couplings. In Sec. III, we apply different c -tagging algorithms for the discovery potential of the cZ' process and discuss fake sources. Sec. IV is dedicated to the bZ' process, and on disentangling the Z' coupling structure by combining with the results of Sec. III. The scenario for having both ccZ' and bbZ' couplings is analyzed in Sec. V, and we summarize in Sec. VI. The analysis for the DY process is detailed in Appendix A.

II. THE DRELL-YAN PROCESS

We take the following effective couplings,

$$\begin{aligned} \mathcal{L} \supset & -g' \left(\bar{\mu}\gamma_\alpha\mu + \bar{\nu}_{\mu L}\gamma_\alpha\nu_{\mu L} - \bar{\tau}\gamma_\alpha\tau - \bar{\nu}_{\tau L}\gamma_\alpha\nu_{\tau L} \right) Z'^\alpha \\ & - \sum_{q=u,d,s}^{c,b} g_{qq}^R \bar{q}_R\gamma_\alpha q_R Z'^\alpha, \end{aligned} \quad (1)$$

where g' is the coupling of Z' to the muon, tauon and their neutrinos, and g_{qq}^R is the right-handed (RH)

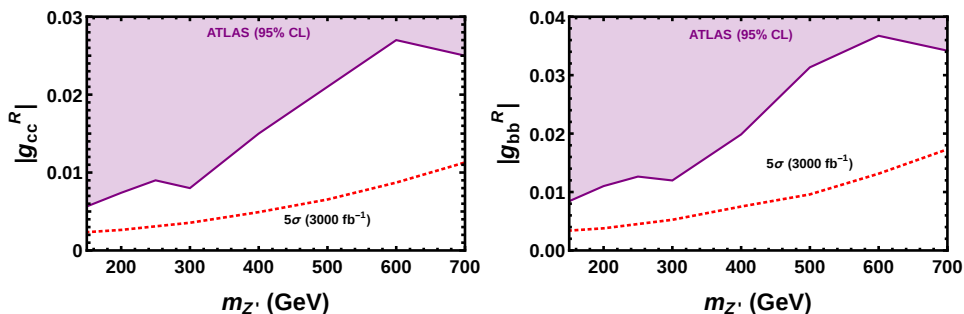


FIG. 1. The 5σ discovery reach of the DY process $pp \rightarrow Z' + X \rightarrow \mu^+\mu^- + X$ at 14 TeV LHC with 3000 fb^{-1} data, initiated by ccZ' (left) and bbZ' (right) couplings. The purple shaded regions are the 95% CL upper limits extracted from Ref. [1].

qqZ' coupling (induced by some underlying heavy particles [9]). The context is the effective model based on the gauged $L_\mu - L_\tau$ [10, 11] symmetry, as discussed in Refs. [9, 12]. For simplicity and to be more general, we set all flavor violating couplings to zero and assume g_{qq}^R to be real. The coupling g' is taken to be much larger than the coupling g_{qq}^R , hence the Z' couples more weakly to quarks, and its decay branching ratios can be approximated as:

$$\mathcal{B}(Z' \rightarrow \mu^+\mu^-) \simeq \mathcal{B}(Z' \rightarrow \tau^+\tau^-) \simeq \mathcal{B}(Z' \rightarrow \nu\bar{\nu}) \simeq \frac{1}{3}. \quad (2)$$

The results in this paper can be scaled to any narrow Z' that couples to quarks and muons by the relation:

$$|g_{qq}^R| \rightarrow |g_{qq}^R| \sqrt{3 \times \mathcal{B}(Z' \rightarrow \mu^+\mu^-)}. \quad (3)$$

Search for heavy dilepton resonances by ATLAS [1] and CMS [2] set stringent bounds on $\sigma(pp \rightarrow Z' + X) \cdot \mathcal{B}(Z' \rightarrow \mu^+\mu^-)$, hence on g_{qq}^R couplings. The ATLAS result is based on 36 fb^{-1} data, while the CMS result is for 13 fb^{-1} . We use the former [1] to extract 95% CL upper limits on g_{cc}^R and g_{bb}^R couplings, shown as the purple shaded regions in Fig. 1. The 5σ discovery reach¹ is given in Fig. 1 with 3000 fb^{-1} data for the High Luminosity LHC (HL-LHC). If the Z' couples to u , d or s quark, the limits on g_{qq}^R would be much stronger due to a larger parton distribution function (PDF), i.e. probing a much smaller g_{uu}^R , g_{dd}^R or g_{ss}^R coupling than that of g_{cc}^R and g_{bb}^R . The details of the cut-based analysis and background processes are given in Appendix A. For sake of a decent S/B ratio, we restrict ourselves to $m_{Z'} \lesssim 700 \text{ GeV}$. Although Eq. (1) is written for effective couplings g_{qq}^R , our results are applicable to left-handed couplings g_{qq}^L , with the replacement $g_{qq}^R \rightarrow g_{qq}^L$.

III. THE cZ' PROCESS

Having discussed the discovery potential of ccZ' coupling through the DY process, we turn to $pp \rightarrow cZ' + X \rightarrow c\mu^+\mu^- + X$, i.e. the cZ' process, which requires tagging of c -jet. Thanks to recent developments in charm tagging by ATLAS [5] and CMS [6], it is now possible to study such a process, where many phenomenological studies and discussions can already be found [13–21].

A. Searching for cZ'

Let us briefly discuss the present c -tagging algorithms. ATLAS [5] gives a range for b - and light-jet rejections² for a fixed value of c -tagging efficiency. These fixed c -tagging efficiencies are presented as curves (called “iso-efficiency curve”) in the b - vs light-jet rejection plane. CMS [6] presents similar constant c -tagging efficiency curves in the b - and light-jet mistag efficiency plane. For ATLAS iso-efficiency curves, c -tagging schemes with high light-jet rejection have low b -jet rejection rates, and vice versa. The CMS curves show similar behavior.

The largest background for the cZ' process is $Z/\gamma^* + \text{light-jet}$. In order to reduce this background, we take two c -tagging working points (WP) with low light-jet mistag rate (i.e. high light-jet rejection) from the ATLAS analysis, which we call configuration 1 (Conf1) and configuration 2 (Conf2), given in the first two rows of Table I. On

	c -tagger	ϵ_c	ϵ_b	ϵ_{light}
ATLAS	Conf1	0.4	0.17	0.1
	Conf2	0.2	0.1	0.004
CMS	ctagL	0.9	0.45	0.99
	ctagM	0.39	0.26	0.19
	ctagT	0.2	0.24	0.02

TABLE I. ATLAS [5] and CMS [6] c -, b - and light-jet tagging efficiencies ϵ_c , ϵ_b and ϵ_{light} for different working points.

¹ Significance is defined by S/\sqrt{B} , where S and B denote the number of signal and background events, respectively.

² The mistag rate is defined as the complement of rejection rate.

<i>c</i> -tagger WP (ATLAS)	Signal	$Z/\gamma^* + c$ -jet	$Z/\gamma^* + b$ -jet	$Z/\gamma^* + \text{light-jet}$	$t\bar{t}$	Wt	WW	WZ	ZZ	Total Bkg.
Conf1	1.34	14.52	3.04	34.66	11.52	1.11	1.35	0.02	0.001	66.22
Conf2	0.67	7.26	1.79	1.39	6.77	0.65	1.59	0.02	0.002	19.47

TABLE II. Signal and background cross sections (in fb) after selection cuts for a 150 GeV Z' (with $g_{cc}^R = 0.005$) produced via $pp \rightarrow cZ' + X \rightarrow c\mu^+\mu^- + X$ at 14 TeV LHC with ATLAS c -tagging schemes, where last column gives total background.

<i>c</i> -tagger WP (CMS)	Signal	$Z/\gamma^* + c$ -jet	$Z/\gamma^* + b$ -jet	$Z/\gamma^* + \text{light-jet}$	$t\bar{t}$	Wt	WW	WZ	ZZ	Total Bkg.
ctagL	3.02	36.31	8.04	343.14	30.48	2.93	3.58	0.11	0.008	420.96
ctagM	1.31	14.16	4.64	65.85	17.61	1.69	2.07	0.03	0.002	106.06
ctagT	0.67	7.26	4.29	6.93	16.26	1.56	1.91	0.03	0.002	38.23

TABLE III. Same as Table. II, but for CMS c -tagging schemes.

the other hand, CMS gives three c -tagging WPs called c -tagger L, M and T (abbreviated as ctagL, ctagM and ctagT in this paper), which we give in the last three rows of Table I. For both ATLAS and CMS, WPs with higher b -jet rejection could be taken at the cost of lower light-jet rejection for a fixed c -tagging efficiency, but we do not consider such cases in this study. Note that these c -tagging schemes show mild dependence on transverse momentum and pseudo-rapidity of the jet. For simplicity, we take them to be constant in this study.

To illustrate the discovery potential of the cZ' process, we choose the benchmark values of mass and coupling

$$m_{Z'} = 150 \text{ GeV}, \quad g_{cc}^R = 0.005,$$

setting all other g_{qq}^R couplings in Eq. (1) to zero.

The cZ' process suffers from several SM backgrounds. The dominant ones are $Z/\gamma^* + \text{jet}$, $t\bar{t}$, Wt , with smaller contributions from WW , WZ and ZZ . There exist non-prompt and fake backgrounds such as $W + \text{jets}$, QCD multi-jets etc., which we do not consider, as these backgrounds are not properly modeled in simulation. Due to different tagging efficiencies and mistag rates, we separate $Z/\gamma^* + \text{jet}$ background into three different categories, i.e. $Z/\gamma^* + c$ -jet, b -jet and light-jet, respectively.

Signal and background events are generated at leading order (LO) in the pp collision with $\sqrt{s} = 14$ TeV via the Monte Carlo event generator MadGraph5_aMC@NLO [22] with the PDF set NN23LO1 [23], interfaced to PYTHIA 6.4 [24] for showering and hadronization. The event samples are finally fed into the fast detector simulator Delphes 3.4.0 [25] for inclusion of (CMS-based) detector effects. We followed MLM matching scheme [26] for matrix element (ME) and parton shower (PS) matching and merging. To take higher order corrections into account, the LO cross section of $Z + \text{light-jet}$ is normalized by a correction factor 1.83 [27] up to NNLO. For simplicity we assume correction factors for the $Z + c$ -jet and $Z + b$ -jet backgrounds to be same as $Z + \text{light-jet}$. The LO $t\bar{t}$ and Wt cross sections are normalized to the NNLO+NNLL ones by factors 1.84 [28] and 1.35 [29], respectively. Furthermore, the LO cross sections of WW , WZ and

ZZ backgrounds are normalized to the NNLO QCD ones by factors 1.98 [30], 2.07 [31] and 1.74 [32], respectively. We do not include K factor for the signal.

We follow Ref. [21] closely in our analysis for both signal and background. Selected events should contain two oppositely charged muons and at least one jet having transverse momenta $p_T^J > 45$ GeV. We require the leading and sub-leading muons to have $p_T^{\mu 1} > 50$ GeV, $p_T^{\mu 2} > 40$ GeV, respectively. The minimum separation between two muons ($\Delta R_{\mu\mu}$) and the separation between any muon and the leading jet ($\Delta R_{\mu j}$) are required to be > 0.4 . The maximum pseudo-rapidity ($|\eta|$) of both muons and the leading jet in an event are required to be < 2.5 . The jets are reconstructed using anti- k_T algorithm with radius parameter $R = 0.5$. To reduce contribution from $t\bar{t}$ and Wt backgrounds, events with missing transverse energy (E_T^{miss}) > 40 GeV are rejected. Finally, we impose an invariant-mass cut $|m_{\mu\mu} - m_{Z'}| < 15$ GeV on the two oppositely charged muons in an event. If an event contains more than one $m_{\mu\mu}$ combination, the combination closest to $m_{Z'}$ is selected. The impact of the selection cuts on the signal and backgrounds are given in Table II (based on ATLAS c -tagging) and Table III (based on CMS c -tagging).

The ATLAS Conf1 and Conf2 schemes may discover cZ' process with 930 fb^{-1} and 1090 fb^{-1} integrated luminosities, respectively. The dominant background contri-

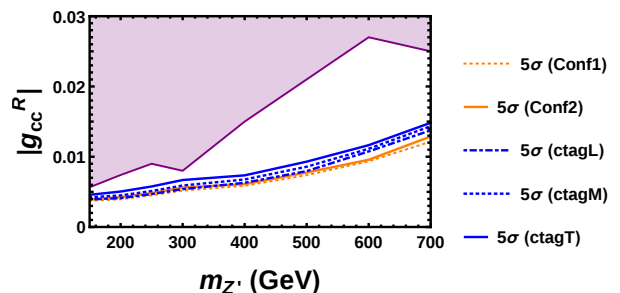


FIG. 2. The 5σ discovery reach of $pp \rightarrow cZ' + X \rightarrow c\mu^+\mu^- + X$ process at 14 TeV with 3000 fb^{-1} data. See text for details.

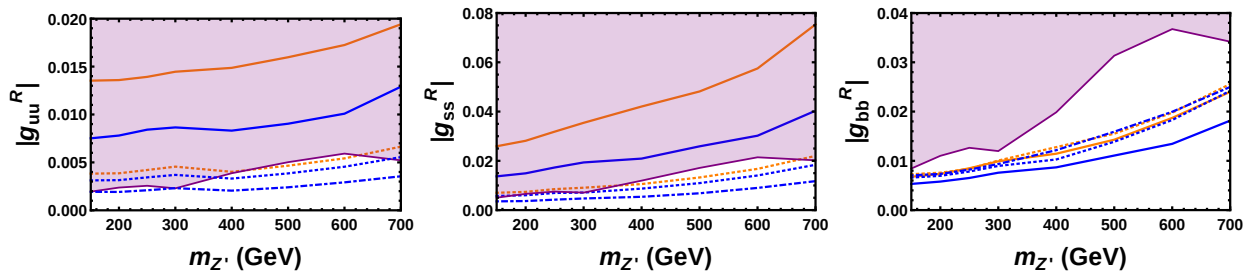


FIG. 3. The 5σ contours of fake cZ' arising from g_{qq}^R coupling at 14 TeV with 3000 fb^{-1} (color schemes as in Fig. 2).

tribution for Conf1 is from $Z/\gamma^* + \text{light-jet}$, while $Z/\gamma^* + c\text{-jet}$ constitute the second largest background. This is distinctly different for Conf2: $Z/\gamma^* + c\text{-jet}$ and $t\bar{t}$ provide the dominant and second largest contributions. A larger c -tagging efficiency makes Conf1 superior to Conf2 for discovery. Similarly, ctagL, ctagM and ctagT for CMS could discover cZ' process with 1150 fb^{-1} , 1550 fb^{-1} and 2120 fb^{-1} integrated luminosities. The ctagL requires roughly the same luminosity as ATLAS Conf2, although the c -tagging efficiencies and b - and light-jet mistag rates are different. The larger c -tagging efficiency of ctagL is balanced by higher mistag rates for light- and b -jets. The smaller c -tagging efficiencies make the cZ' process harder to discover for ctagM and ctagT.

Following the same selection cuts, we extend our analysis for Z' mass up to 700 GeV. The discovery reaches for the ATLAS Conf1 (orange dotted), Conf2 (orange solid), CMS ctagL (blue dot-dashed), ctagM (blue dotted) and ctagT (blue solid) with 3000 fb^{-1} data are given in Fig. 2.

B. Fake cZ'

Signal for cZ' process could arise from light- and b -jet mistags, which we display in Fig. 3 for the cases of g_{uu}^R (left), g_{ss}^R (middle) and g_{bb}^R (right) couplings, for LHC at $\sqrt{s} = 14 \text{ TeV}$ with 3000 fb^{-1} data. The purple shaded regions correspond to 95% CL upper limits extracted from Ref. [1]. Let us take a closer look.

The fake cZ' signals depend on the upper limits on qqZ' coupling and the c -tagging schemes adopted. The extraction of upper limits involves the underlying DY process $q\bar{q} \rightarrow Z'$, which depends on the initial state quark PDFs, and is also proportional to $|g_{qq}^R|^2$. On the other hand, fake cZ' signals can originate from $qg \rightarrow qZ'$ and its conjugate process. Although also proportional to $|g_{qq}^R|^2$, the cross sections are suppressed by the $2 \rightarrow 2$ nature compared to the DY process, and depend on gluon and quark PDFs. Due to high light-jet rejection rates, two c -tagging schemes Conf2 and ctagT can fully eliminate fake cZ' from light-jets. That is, the 5σ contours for them lie in the excluded regions for both g_{uu}^R and g_{ss}^R couplings in the Z' mass range studied, unlike Conf1, ctagL and ctagM, which excludes only some $m_{Z'}$ regions.

None of these schemes, however, shows promise in

reducing fakes from b -jet misidentification, since all schemes have considerable b -jet mistag rates. This can be seen from the rightmost panel of Fig. 3. The high light-jet rejection and low c -tagging efficiency (to reduce the dominant $Z/\gamma^* + \text{light-}$ and $Z/\gamma^* + c\text{-jet}$ backgrounds) make ctagT performing the worst. However, although having same c -tagging efficiency and even lower light-jet rejection, the lower b -jet mistag rate of Conf2 makes it perform better than ctagT. Our choice of high light-jet, but moderate b -jet, rejections allows the possibility of fake cZ' arising from bbZ' coupling. We thus turn to scrutinize this issue in the next section.

IV. THE bZ' PROCESS

A. Searching for bZ'

If the discovery of DY produced Z' is due to bbZ' coupling, it implies $bg \rightarrow bZ' \rightarrow b\mu^+\mu^-$ (and its conjugate) could also be discovered at the LHC. To illustrate the potential for $pp \rightarrow bZ' + X \rightarrow b\mu^+\mu^- + X$ at LHC, we adopt similar strategy as before, and take the following benchmark for mass and coupling:

$$m_{Z'} = 150 \text{ GeV}, \quad g_{bb}^R = 0.005.$$

We follow the same cut-based analysis as in previous section, except the tag jet is now a b -jet. We incorporate in Delphes p_T and η dependent b -tagging efficiencies. The rejection factor of the light-jets are taken as 137 [37]. For simplicity, we assume the correction factors to the LO background cross sections generated by MadGraph to be the same as in previous section, and do not multiply K factor for the signal. The signal and background cross sections after selection cuts are given in Table IV. The required luminosity to discover the 150 GeV Z' is 1180 fb^{-1} . Our analysis is further extended up to $m_{Z'} = 700 \text{ GeV}$, as shown in the left panel of Fig. 4.

B. Fake bZ'

Mistagged light- or c -jets can also produce fake bZ' signals at the LHC, but the required g_{qq}^R couplings ($q =$

Signal	$Z/\gamma^* + b\text{-jet}$	$Z/\gamma^* + c\text{-jet}$	$Z/\gamma^* + \text{light-jet}$	$t\bar{t}$	Wt	WW	WZ	ZZ	Total Bkg.
1.31	11.35	6.89	2.53	53.21	4.28	2.69	0.001	0.0001	80.95

TABLE IV. Signal and background cross sections (in fb) after selection cuts for a 150 GeV Z' (with $g_{bb}^R = 0.005$) via $pp \rightarrow bZ' + X \rightarrow b\mu^+\mu^- + X$ (plus conjugate process) at 14 TeV LHC.

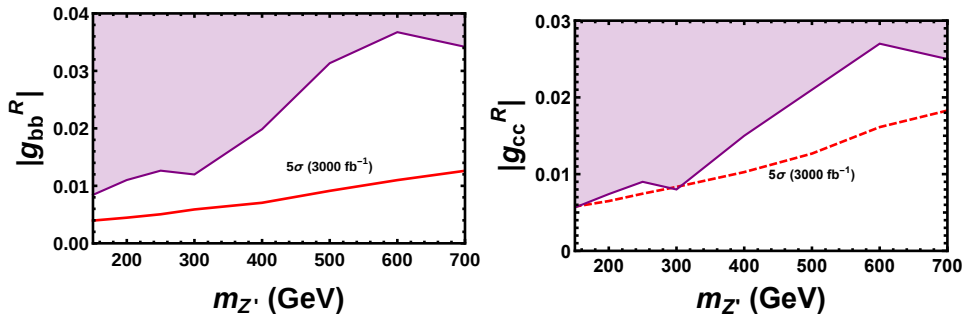


FIG. 4. Discovery reach of bZ' originating from g_{bb}^R (left) and g_{cc}^R (right) couplings at 14 TeV LHC with 3000 fb^{-1} data.

u, d, s) to produce fake bZ' at 5σ with 3000 fb^{-1} are already disallowed by heavy resonance DY searches [1]. This attests to the excellent performance of b -tagging algorithms in reducing light-jet contributions. However, fake bZ' can still arise from mistagged c -jets, except two tiny mass windows around $m_{Z'} \sim 150$ and 300 GeV , as can be read from the right panel of Fig. 4 for the 5σ reach with 3000 fb^{-1} . We infer that, if no Z' is observed via DY with $\sim 250 \text{ fb}^{-1}$ dataset, one can rule out the possibility of fake bZ' from the ccZ' coupling at LHC.

Even if a Z' is discovered via DY with $\sim 100 \text{ fb}^{-1}$ or smaller dataset, one can still eliminate the possibility of fake bZ' from ccZ' coupling by combining bZ' and cZ' searches. For instance, a 600 GeV Z' with $g_{cc}^R = 0.02$, which can be discovered with 110 fb^{-1} data via DY, requires 1310 fb^{-1} data to give fake bZ' at 5σ , while observing cZ' does not take long after the discovery of DY (e.g. 160 fb^{-1} for Conf2 and 350 fb^{-1} for ctagT; see the left panel of Fig. 1, Fig. 2, and right panel of Fig. 4). In general, fake bZ' from ccZ' coupling, if observed, should be preceded by the discovery of cZ' with a smaller dataset. A similar argument holds for fake cZ' from bbZ' coupling: after discovery via DY induced by bbZ' , fake cZ' can emerge, but it should be preceded by discovery of bZ' for all five c -tagging schemes (see the right panels of Fig. 1 and Fig. 3, and left panel of Fig. 4). Therefore, the simultaneous search for cZ' and bZ' can reveal if the coupling behind DY production is ccZ' or bbZ' .

V. PRESENCE OF BOTH cZ' AND bZ' PROCESSES

We have so far studied the discovery potential of cZ' and bZ' processes with a nonzero ccZ' or bbZ' coupling exclusively. However, all uuZ' , ddZ' , ssZ' , ccZ' and bbZ' couplings could in principle coexist. If any of the first three couplings involving light quarks are nonzero, we

might discover Z' in DY process, without subsequent discovery of cZ' and/or bZ' processes which can be easily discerned by using both c - and b -tagging algorithms.

A more interesting scenario is when both ccZ' and bbZ' couplings are nonzero, but all other couplings to light quarks vanish. These couplings would give rise to both cZ' and bZ' processes, depending on their individual strengths. In order to investigate such a scenario, we take the following benchmark point:

$$m_{Z'} = 150 \text{ GeV}, g_{cc}^R = 0.003, g_{bb}^R = 0.005.$$

These g_{cc}^R and g_{bb}^R values remain within respective allowed regions, as well as $\sigma(pp \rightarrow Z' + X) \cdot \mathcal{B}(Z' \rightarrow \mu^+\mu^-)$ within 95% CL upper limit set by ATLAS [1]. Larger g_{cc}^R and g_{bb}^R would be in tension with $\sigma \cdot \mathcal{B}$ upper limit.

This benchmark can be discovered in the DY process with just 210 fb^{-1} integrated luminosity, followed by a discovery in the bZ' process with 870 fb^{-1} data, which is lower than the one quoted for case $g_{bb}^R = 0.005$ alone in Sec. IV A. The cZ' process would emerge later, at 2370 fb^{-1} (Conf1), 2420 fb^{-1} (Conf2), 2570 fb^{-1} (ctagL), 2600 fb^{-1} (ctagM) or 1740 fb^{-1} (ctagT). The benchmark thus illustrates the possibility of uncovering both charm and bottom couplings of a new Z' resonance, and the efficacy of the HL-LHC. Further sharpening of heavy flavor tagging tools would be helpful.

VI. SUMMARY

We analyze the possibility to probe the coupling structure of a relatively weakly coupled Z' via the $q\bar{q} \rightarrow qZ'$ process, adopting c - and b -tagging algorithms of ATLAS and CMS at 14 TeV LHC. Such a resonance would appear first in the Drell-Yan process. Our study shows that, if a Z' is discovered first via the $pp \rightarrow Z' + X \rightarrow \mu^+\mu^- + X$ DY production, one could then discover $cg \rightarrow cZ'$ and

$bg \rightarrow bZ'$ processes at the HL-LHC. We illustrate with two different c -tagging schemes from ATLAS, chosen to optimally reduce Z + light-jet background, but maintaining moderate c -tagging efficiencies. We also adopt three c -tagging working points from CMS in our analysis.

The cZ' process could arise from misidentification of light- or b -jets. Fake cZ' from light-jet misidentification can be excluded by existing data, if one adopts ATLAS Conf2 or CMS ctagT scheme. However, none of the c -tagging schemes can rule out the possibility of fake cZ' from mistag of b -jets. In order to eliminate fake cZ' from finite bbZ' coupling, we advocate simultaneous study of cZ' and bZ' processes. We find that a nonzero bbZ' coupling would give genuine bZ' and fake cZ' signatures. Conversely, a nonzero ccZ' coupling can give genuine cZ' and fake bZ' , within the allowed region of ccZ' coupling. The latter possibility can be eliminated in the near future if no Z' emerges in the DY process with $\sim 250 \text{ fb}^{-1}$ data. Our study is based on the current status of c -tagging algorithms. Any future improvement in c -tagging would only improve the analysis.

It would be interesting if both ccZ' and bbZ' couplings are nonzero. We illustrate with one such representative scenario, i.e. for a 150 GeV Z' with $g_{cc}^R = 0.003$ and $g_{bb}^R = 0.005$. We find that 210 fb^{-1} data is needed for DY discovery, which would be followed by discovery of the bZ' process with 870 fb^{-1} , while the cZ' process would emerge much later with integrated luminosities ranging from $\sim 1740 \text{ fb}^{-1}$ to 2600 fb^{-1} , depending on c -tagging scheme. This scenario differs from cases when either g_{cc}^R or g_{bb}^R vanish. For example, when only $g_{cc}^R = 0.005$ is nonzero, DY discovery for a 150 GeV Z' would be followed by discovery in the cZ' process, without emergence of subsequent 5σ signature of fake bZ' process, even with full HL-LHC data. However, if $g_{bb}^R = 0.005$ is the only nonzero coupling, DY process would be followed by discovering the bZ' process. The highest attainable fake cZ' signature in this scenario would be about 4.4σ . We have not included systematic uncertainties, backgrounds associated with fake and nonprompt sources, and QCD corrections for the signal, which would induce some uncertainties to our estimated integrated luminosities for discovery.

Our study illustrates that new resonances could still emerge at the LHC, and large integrated luminosities can

probe weaker couplings, or unravel more detail. Given that our study was partly motivated by flavor ‘‘anomalies’’, associated flavor of Z' production could shed more light on potential new physics indications from the flavor sector. Of course, one would certainly search for other Z' decay modes, such as $Z' \rightarrow \tau^+\tau^-$ implied by Eq. (1).

ACKNOWLEDGMENTS

This work is supported by grants NTU-ERP-106R8811 and NTU-ERP-106R104022, and MOST 105-2112-M-002-018, 106-2811-M-002-187 and 106-2112-M-002-015-MY3. WSH thanks G.N. Taylor for hospitality.

Appendix A: Signal and background for DY process

The dominant backgrounds associated with DY production are the Z/γ^* and $t\bar{t}$ processes, with subdominant contributions from Wt and VV productions, where $V = W, Z$. Selected events should contain two oppositely-charged muons with transverse momenta $p_T^\mu > 50 \text{ GeV}$, and an invariant-mass cut of $|m_{\mu\mu} - m_{Z'}| < 15 \text{ GeV}$ is imposed. Signal and background processes are generated at LO via MadGraph5_aMC@NLO, interfaced to PYTHIA 6.4 and fed into fast detector simulator Delphes 3.4.0, following the MLM prescription for the ME and PS matching and merging. The QCD correction factors for the $t\bar{t}$, Wt and VV backgrounds are the same as described in Sec. III. However, the Z/γ^* cross section is corrected up to NNLO QCD +NLO EW by a factor 1.27, obtained by FEWZ 3.1 [38]. The impact of the selection cuts on different backgrounds are given in Table. V for various Z' masses. Note that, just like cZ' and bZ' processes, we do not include K factor for the signal.

$m_{Z'}$ (GeV)	150	200	300	400	500	600	700
Total Bkg.	2311	838	177	55	20	9	5

TABLE V. Background cross sections (in fb) for the DY process after selection cuts, for various $m_{Z'}$ values.

-
- [1] M. Aaboud *et al.* [ATLAS Collaboration], JHEP **1710**, 182 (2017) [arXiv:1707.02424 [hep-ex]]. The $\sigma(pp \rightarrow Z' + X) \cdot \mathcal{B}(Z' \rightarrow \mu^+\mu^-)$ 95% CL upper limit is available, along with other auxiliaries, at <https://atlas.web.cern.ch/Atlas/GROUPS/PHYSICS/PAPERS/EXO-2016-05/>.
- [2] CMS Collaboration, CMS-PAS-EXO-16-031.
- [3] W.-S. Hou, M. Kohda and T. Modak, Phys. Rev. D **96**, 015037 (2017) [arXiv:1702.07275 [hep-ph]].
- [4] ATLAS Collaboration, ATLAS-PHYS-PUB-2015-001.
- [5] ATLAS Collaboration, ATLAS-PHYS-PUB-2017-013.
- [6] CMS Collaboration, CMS-PAS-BTV-16-001.
- [7] G. Aad *et al.* [ATLAS Collaboration], JINST **11**, P04008 (2016) [arXiv:1512.01094 [hep-ex]].
- [8] CMS Collaboration, CMS-PAS-BTV-15-001.
- [9] K. Fuyuto, W.-S. Hou and M. Kohda, Phys. Rev. D **93**, 054021 (2016) [arXiv:1512.09026 [hep-ph]].
- [10] X.G. He, G.C. Joshi, H. Lew and R.R. Volkas, Phys. Rev. D **43**, 22 (1991).
- [11] R. Foot, Mod. Phys. Lett. A **6**, 527 (1991).

- [12] W. Altmannshofer, S. Gori, M. Pospelov and I. Yavin, Phys. Rev. D **89**, 095033 (2014) [arXiv:1403.1269 [hep-ph]].
- [13] C. Delaunay, T. Golling, G. Perez and Y. Soreq, Phys. Rev. D **89**, 033014 (2014) [arXiv:1310.7029 [hep-ph]].
- [14] G. Perez, Y. Soreq, E. Stamou and K. Tobioka, Phys. Rev. D **92**, 033016 (2015) [arXiv:1503.00290 [hep-ph]]; *ibid.* D **93**, 013001 (2016) [arXiv:1505.06689 [hep-ph]].
- [15] I. Brivio, F. Goertz and G. Isidori, Phys. Rev. Lett. **115**, 211801 (2015) [arXiv:1507.02916 [hep-ph]].
- [16] G.W.-S. Hou [ATLAS and CMS Collaborations], PoS CHARM **2016**, 088 (2016).
- [17] S. Iwamoto, G. Lee, Y. Shadmi and Y. Weiss, JHEP **1709**, 114 (2017) [arXiv:1703.05748 [hep-ph]].
- [18] T. Han and X. Wang, JHEP **1710**, 036 (2017) [arXiv:1704.00790 [hep-ph]].
- [19] T. Cohen, M. Freytsis and B. Ostdiek, arXiv:1706.09451 [hep-ph].
- [20] U. Haisch, arXiv:1706.09730 [hep-ph].
- [21] A. M. Sirunyan *et al.* [CMS Collaboration], arXiv:1711.02143 [hep-ex].
- [22] J. Alwall *et al.*, JHEP **1407**, 079 (2014) [arXiv:1405.0301 [hep-ph]].
- [23] R.D. Ball *et al.* [NNPDF Collaboration], Nucl. Phys. B **877**, 290 (2013).
- [24] T. Sjöstrand, S. Mrenna and P. Z. Skands, JHEP **0605**, 026 (2006) [hep-ph/0603175].
- [25] J. de Favereau *et al.* [DELPHES 3 Collaboration], JHEP **1402**, 057 (2014) [arXiv:1307.6346 [hep-ex]].
- [26] J. Alwall *et al.*, Eur. Phys. J. C **53**, 473 (2008) [arXiv:0706.2569 [hep-ph]].
- [27] R. Boughezal, X. Liu and F. Petriello, Phys. Rev. D **94**, 074015 (2016) [arXiv:1602.08140 [hep-ph]].
- [28] ATLAS-CMS recommended predictions for top-quark-pair cross sections: <https://twiki.cern.ch/twiki/bin/view/LHCPhysics/TtbarNNLO>.
- [29] N. Kidonakis, Phys. Rev. D **82**, 054018 (2010) [arXiv:1005.4451 [hep-ph]].
- [30] T. Gehrmann *et al.*, Phys. Rev. Lett. **113**, 212001 (2014) [arXiv:1408.5243 [hep-ph]].
- [31] M. Grazzini, S. Kallweit, D. Rathlev and M. Wiesemann, Phys. Lett. B **761**, 179 (2016) [arXiv:1604.08576 [hep-ph]].
- [32] F. Cascioli *et al.*, Phys. Lett. B **735**, 311 (2014) [arXiv:1405.2219 [hep-ph]].
- [33] R. Aaij *et al.* [LHCb Collaboration], Phys. Rev. Lett. **111**, 191801 (2013) [arXiv:1308.1707 [hep-ex]].
- [34] R. Aaij *et al.* [LHCb Collaboration], JHEP **1602**, 104 (2016) [arXiv:1512.04442 [hep-ex]].
- [35] R. Aaij *et al.* [LHCb Collaboration], Phys. Rev. Lett. **113**, 151601 (2014) [arXiv:1406.6482 [hep-ex]].
- [36] ATLAS Collaboration, ATLAS-CONF-2017-027.
- [37] ATLAS Collaboration, ATLAS-CONF-2014-058.
- [38] Y. Li and F. Petriello, Phys. Rev. D **86**, 094034 (2012) [arXiv:1208.5967 [hep-ph]].